Nature Environment and Pollution Technology
An International Quarterly Scientific Journal

p-ISSN: 0972-6268
(Print copies up to 2016)
e-ISSN: 2395-3454

Vol. 24 | No. 2 | Article ID B4242 | 2025

Original Research Paper

https://doi.org/10.46488/NEPT.2025.v24i02.B4242

Open Access Journal

Sustainable Phosphate Removal with Acid-Modified Fly Ash: Kinetic, Isothermal, and Thermodynamic Insights

Renu Bala[1], Rajesh Dhankhar[2] and Sunil Kumar Chhikara[1]†

[1]University Institute of Engineering & Technology, Maharshi Dayanand University, Rohtak-124001, Haryana, India
[2]Department of Environmental Science, Maharshi Dayanand University, Rohtak, Haryana, India
†Corresponding Author: Sunil Kumar Chhikara; sunilchhikara.uiet@mdurohtak.ac.in

Abbreviation: Nat. Env. & Poll. Technol.
Website: www.neptjournal.com

Received: 27-06-2024
Revised: 09-08-2024
Accepted: 28-08-2024

Key Words:

Adsorption isotherms
Acid-modified fly ash
Phosphate removal
Chemical kinetics

ABSTRACT

The removal of pollutants from water bodies has emerged as a pressing global concern. Discharging untreated wastewater into the environment poses a significant threat due to the presence of hazardous substances like nitrate and phosphate, contributing to the widespread issue of eutrophication. This study focused on investigating the adsorption of phosphate from a synthetic solution using fly ash, an industrial by-product. To enhance the efficiency of coal fly ash, acid treatment was employed. Batch experiments were conducted to examine the influence of different factors, including pH, adsorbent dosage, initial phosphate ion concentration, contact time, and temperature. Surface electron microscopy (SEM) explained the morphology of the adsorbent, and Fourier Transform Infrared Spectroscopy (FTIR) analysis was performed to analyze the adsorbent pre and post-adsorption, allowing for the identification of functional groups tangled in the adsorption process. The major functional groups observed were hydroxyl, carboxylic acid, amines, and nitrile groups, all contributing to the adsorption process. Acid-modified fly ash (AMFA) demonstrated favorable results in terms of phosphate removal, particularly at a pH of 5.0 and an initial phosphate concentration of 50 ppm. Equilibrium in adsorption was achieved within 30 min at a temperature of 15°C with constant stirring of 100 rpm, resulting in a high phosphate removal rate of 91%. Freundlich isotherm was found to contribute a better fit for the adsorption data compared to the Langmuir isotherm. Pseudo-second-order kinetic model, with a high R^2 value of 0.998, exhibited excellent agreement with the adsorption data for acid-modified fly ash. Thermodynamic study indicated that the adsorption process was heat absorbing (endothermic) and non-spontaneous at low temperatures. Overall, the results of the experimental study highlighted the promising adsorption potential of acid-modified fly ash as an effective adsorbent for phosphate removal in water treatment applications.

Citation for the Paper:

Renu Bala, Dhankhar, R. and Chhikara, S. K., 2025. Sustainable phosphate removal with acid-modified fly ash: Kinetic, isothermal, and thermodynamic insights. *Nature Environment and Pollution Technology*, 24(2), p. B4242. https://doi.org/10.46488/NEPT.2025.v24i02.B4242

Note: From year 2025, the journal uses Article ID instead of page numbers in citation of the published articles.

INTRODUCTION

Phosphorus is a crucial nutrient for plants, animals, and humans. When phosphorus-based substances are extensively used in industry, livestock, and agriculture, they inevitably lead to the release of phosphate into surface water. This discharge has the potential to stimulate the overgrowth of algae, giving rise to algal blooms that endanger the integrity of surface and groundwater, as well as human health (Recepoglu et al. 2022). Phosphate discharge into surface waters excites the proliferation of aquatic micro and macro organisms, leading to an overabundance that can result in eutrophication in stagnant water bodies. Eutrophication is a global environmental concern that has severe consequences for aquatic ecosystems, such as biodiversity loss and significant economic losses (Zhou et al. 2022). Therefore, it is essential to adhere to phosphate discharge limits, which range from 0.5 to 1.0 $mg.L^{-1}$, for waste materials containing phosphates (Ragheb 2013). Despite efforts made over the past few decades to reduce phosphorus pollution in water systems from various environmental sources, water pollution caused by phosphorus remains a significant environmental issue (Park et al. 2021).

A wide array of technologies has been extensively studied for phosphorus removal from wastewater, mainly classified into chemical, biological, and physical methods (Karaca et al. 2004, Wang et al. 2012). However, chemical methods often lead to the formation of substantial sludge during phosphorus precipitation, which may raise new-fangled pollution concerns (Yao et al. 2011, Yeoman et al. 1988). On the other hand, biological methods are effective but sensitive to operational parameters, leading to variable efficiency (Sun et al. 2017, Xie et al. 2017). Additionally, biological treatment requires extra steps like waste-activated sludge disposal or pre-treatment, which can escalate the overall price value of wastewater treatment (Neufeld & Thodos 1969, Yang et al. 2018). Physical methods for wastewater treatment include electrodialysis, reverse osmosis, and adsorption (Loganathan et al. 2014). These techniques are utilized to remove various pollutants and contaminants from water, providing effective purification and treatment of wastewater. However, these methods are limited by the risk of secondary contamination, strict reaction requirements, large space, less flexibility, and design, which involve higher costs (Yin et al. 2017).

Among all of these, adsorption is considered a better wastewater treatment process. The utilization of adsorption as a water purification technology offers several advantages, including its relatively low cost and reduced risks of causing secondary pollution. As a result, it holds great potential for on-site water treatment applications. However, a key factor in successfully implementing adsorption on a large scale is the advancement of affordable and highly efficient adsorbents specifically designed for the removal of phosphate from water (Saad Algarni & Al-Mohaimeed 2022). In modern years, various studies have been performed to estimate the efficiency of low-cost adsorbents for the confiscation of various pollutants (De Gisi et al. 2016).

Recently, a fresh and all-encompassing strategy has been developed, incorporating the principles of the circular economy paradigm. This approach focuses on the reclamation of agricultural and industrial waste derivatives, utilizing them to create innovative composite materials aimed at purifying the environment, particularly with a strong emphasis on rejuvenating water resources (Xu et al. 2022). Industrial waste is highly appealing as a potentially economical adsorbent for wastewater treatment due to its ability to efficiently remove pollutants. It often requires minimal processing to enhance its adsorptive capacity, making it an attractive option for sustainable and economical treatment methods. Different forms of industrial wastes, like red mud, lignin, iron (III) hydroxide, blast furnace sludge, waste slurry, and fly ash, have been investigated for their mechanical viability in commendably removing pollutants from contaminated water (Ahmaruzzaman 2011).

Coal fly ash is a significant industrial waste product generated from the burning of coal and is produced in substantial quantities worldwide. Unfortunately, this waste material poses numerous environmental challenges, including the contamination of soil and water, along with issues related to resource recovery (Usman et al. 2023). Various approaches have been suggested for the sustainable management of coal fly ash. These strategies involve utilizing coal fly ash in different industries, including the cement industry (Singh et al. 2019), rubber production (Ren & Sancaktar 2019), as well as engineering and agricultural applications (Ahmaruzzaman 2010). Moreover, due to its remarkable potential as a phosphate adsorbent, effective recovery of phosphorus from wastewater can be considered a valuable alternate approach to employing coal fly ash (Hosseinpour et al. 2023). The unmodified adsorbent possesses closed pores on its surface (Wulandari et al. 2019). To address this issue and increase the accessibility of the pores, a modification process is necessary. One such modification involves using acid-modified fly ash, which can dissolve impurity minerals present in the fly ash. This dissolution process leads to the widening of the fly ash pores, as the exchanged cation in the fly ash structure is replaced by H^+ ions (Irawan et al. 2014). This modification technique enables the opening of previously closed pores (Wulandari et al. 2019). Recent research on modified fly ash has shown its effectiveness as an adsorbent for a range of pollutants, emphasizing its potential role in environmental remediation. Various studies have been conducted using modified fly ash to remove ammonia (Wang et al. 2024), methylene blue dye (Küçük & Üstündağ 2024), and copper (Buema et al. 2021) from aqueous solutions under optimal conditions, while many studies have explored the removal of phosphate using unmodified fly ash, relatively few have specifically investigated the effectiveness of fly ash after modification. This highlights the need for further research to fully understand the potential of modified fly ash as an efficient adsorbent for phosphate removal.

In the present study, fly ash is improved with acid to enhance its adsorption capacity so that it can be considered as a worthy adsorbent material for the adsorption of phosphate as aluminum, iron, and calcium oxides enrich fly ash. Together with phosphate, these oxides can precipitate or adsorb aggressively. The purpose of the study is to perform acid-modified fly ash as an adsorbent for the removal of phosphate adsorption from synthetic solutions in batch mode studies. Results achieved from batch experiments were subsequently utilized to determine adsorption kinetics, isotherms, and thermodynamics. These analyses helped to understand the rate of adsorption, equilibrium relationships between adsorbate and adsorbent, and the thermodynamic feasibility of the adsorption process.

MATERIALS AND METHODS

All of the chemicals employed in the experiment were of analytical grade. Potassium dihydrogen phosphate (KH_2PO_4) was taken to prepare the stock solution of phosphate. Various working solutions with varying concentrations were equipped by diluting the original phosphate solution using de-ionized water. A pH meter (Mettler Toledo Fiveeasy Plus) was used to determine the solution's pH. To achieve the desired pH levels during the batch studies, 1N solutions of sodium hydroxide (NaOH) and hydrochloric acid (HCl) were used for pH adjustment. Ammonium molybdate and stannous chloride were used as reagents for the phosphate solutions.

Preparation of the Adsorbent

In the current study, fly ash was obtained from the thermal power plant located in Khukhrana, Panipat, Haryana, at coordinates 29°23'50" N and 76°52'52" E. To prepare the fly ash for subsequent experiments, it was initially filtered via a sieve with mesh dimensions of 150 µm. Manual washing of the fly ash was performed using double distilled water, repeating the process 5-7 times to ensure thorough cleaning. Following the washing step, the fly ash was desiccated at 100°C for 24 h to eliminate remaining moistness. The dried-out fly ash was then stored in hermetic containers to preserve its properties. Subsequently, the fly ash was further modified into acid-modified fly ash for subsequent use in the study.

Preparation of Acid Modified Fly Ash (AMFA) as an Adsorbent

During the modification process, fly ash was thoroughly mixed with 1 M HCl solution. The mixture was then placed in a shaker and agitated at 80 °C for 24 h, with a rotation speed of 50 RPM. After the agitation period, the solid was separated by centrifugation, and excess HCl was eliminated through washing with double distilled water. The resulting product was referred to as acid-modified fly ash. It was subsequently dried at 105°C for 24 h to ensure complete removal of moisture. The modified adsorbent was considered ready for use in adsorption experiments and was stored in hermetic containers to maintain its properties.

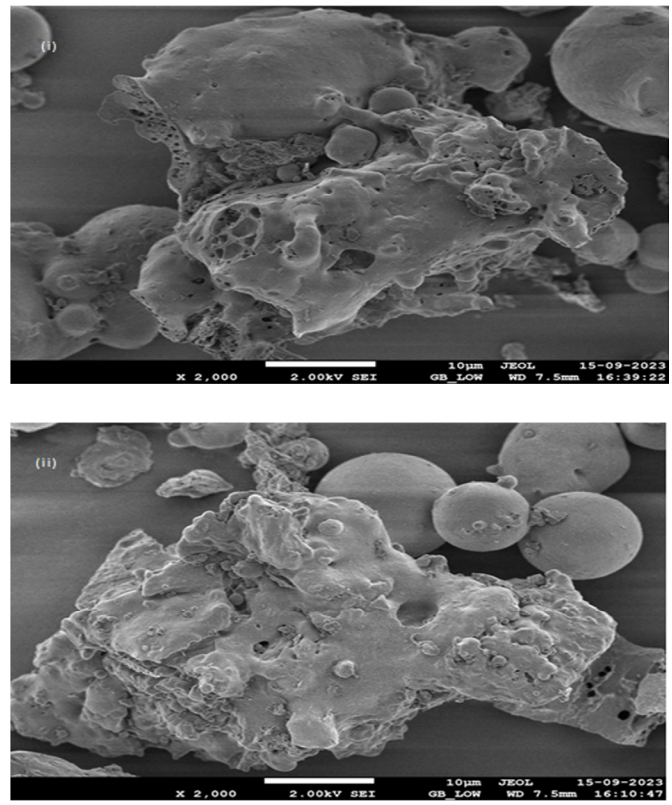

Fig. 1: Surface Morphology of AMFA (i) before phosphate adsorption (ii) after phosphate adsorption.

RESULTS AND DISCUSSION

Characterization of Adsorbents

SEM analysis: The surface morphology of AMFA before and after adsorption is shown in Fig. 1 (i & ii). It was noticed that before adsorption, the AMFA surface was porous with some spherical and irregular structures. However, after phosphate adsorption, it showed agglomeration of phosphate ions and filling of binding sites with improvement in the surface of the structure.

FTIR analysis: The functional groups present on the adsorbent were detected using FTIR (Bruker Alpha, Department of Biotechnology, UIET, MDU) spectrometer having wavelength region 400-4000 cm^{-1} before and after phosphate adsorption.

FTIR results for unadsorbed and adsorbed adsorbents are presented in Fig. 2 (i) & (ii), indicating the presence of hydroxyl, carboxylic acid, amines, and nitrile groups. These functional groups have been identified on the surface of AMFA before and after phosphate adsorption. The substantial peaks were noticed at approximately 1079.24, 788.29, 641.59 cm^{-1}. The FTIR spectrum of phosphate ion adsorption resulted in peaks at 1079.24 attributed to PO_4^{3-}, 788.29, 641.59 cm^{-1} representing the symmetric stretching of the Si–O–Si and Al–O–Si band. It was perceived that peak formation in FTIR spectra changed after phosphate

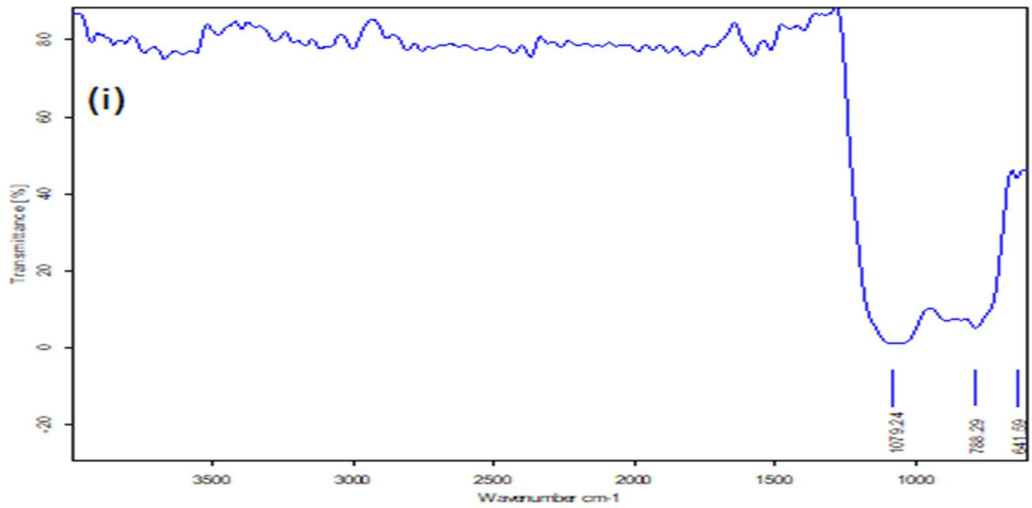

Fig. 2: (i) Raw adsorbent (AMFA) (Unadsorbed)

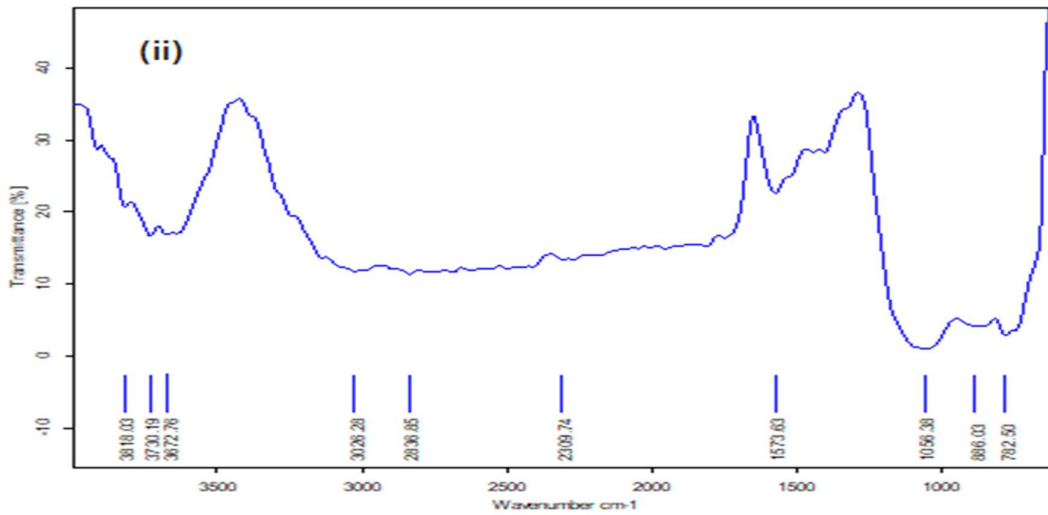

Fig. 2: (ii) AMFA (Adsorbed)

adsorption and indicated that phosphate ions after adsorption enhanced the function group count. After adsorption (Fig. 2. ii) more peaks were noticed in the spectra at 3818.03, 3730.019, 3672.76, 3026.28, 2836.85, 2309.74, 1573.63, 1056.38, 886.03, 782.50 which represent single bend stretch, non-bonded O-H stretching (OH group), O-H stretching vibration, nitriles, amides, amines, peak at 1056.38 represent the peak shifting from 1079.24 indicating phosphate adsorption taken on the surface of adsorbent.

Phosphate Removal Experiments

To investigate the effects of various parameters on the removal of phosphate from synthetic solutions, a batch process was conducted. The experiment was performed in conical flasks of 100 mL, where 50 mL of a known phosphate concentration was taken. The adsorbent dosage used was 0.5 g, and the pH was adjusted accordingly by using 1N HCl and 1N NaOH. A mechanical shaker was employed during the batch study, operating at 100 RPM at a temperature of 25°C. The samples were agitated for one hour. After the completion of the agitation period, the conical flasks were taken out from the shaker and kept outside at room temperature to settle for 2-3 min to allow the adsorbents to separate from the solution. The solution was filtered using Whatman filter paper no. 1, followed by filtrate analyzed by using ammonium molybdate and stannous chloride as reagents, which gave a blue color to the solution (APHA 2012). After the color development, the concentration of phosphate was measured at 690 nm wavelength using a UV-spectrophotometer (UV-1800 Shimazu).

The following equation was used to calculate the uptake capacity:

$$\text{Uptake capacity } (q_e) = \frac{C_i - C_e}{m} \times V \quad \ldots(1)$$

wherein q_e depicts the quantity of phosphate adsorbed at equilibrium ($mg.g^{-1}$), C_i and C_e depict the initial and final concentration of phosphate ions ($mg.L^{-1}$), V depicts the volume of phosphate solution

(L), m depicts the quantity of adsorbent (g).

Removal efficiency (%) of phosphate ion was calculated using Eq (2) as follows:

$$\text{Removal efficiency } (\%) = \frac{C_i - C_e}{C_i} \times 100 \quad \ldots(2)$$

where C_i and C_e denote the initial and final phosphate ion concentrations.

Isotherms, Kinetics, and Thermodynamics Studies

For the evaluation of adsorption data, Langmuir, Freundlich, and Temkin isotherm models were employed. Kinetics evaluation provided different sorts of sorption mechanisms. The adsorption kinetics are explained with the help of pseudo-first-order and pseudo-second-order kinetic equations. The adsorption capacity of the adsorbate on any porous medium is determined by intra-particle diffusion, a secondary procedure that evaluates adsorption uptake capacity using the square root of time. From temperature-dependent data, calculations were conducted to ascertain the thermodynamic quantities, including enthalpy change (ΔH°), entropy change (ΔS°), and free energy change (ΔG°), linked to the sorption of phosphate on acid-modified fly ash (AMFA).

Batch Experiments

Adsorption encompasses the creation of an adsorbate layer on the adsorbent's surface. This phenomenon can take place through both physical and chemical mechanisms. In physiosorption, the adsorbate molecules in a solution create a deposit on the adsorbent surface due to Van der Waals forces of attraction. On the other hand, chemical adsorption involves the formation of a molecular layer of the adsorbate through chemical reactions on the surface (Sharma et al. 2016). The presence of functional groups such as hydroxyl and carboxyl significantly improves the binding efficiency of modified fly ash for a variety of pollutants, with adsorption behavior typically described by isotherm models that indicate monolayer and multilayer adsorption on adsorption binding sites. Environmental factors, including pH, temperature, and pollutant concentration, greatly affect the adsorption process, highlighting the necessity of optimizing both modification techniques and operational parameters to enhance the effectiveness of modified fly ash in environmental remediation applications. Many studies collectively provide evidence for the adsorption mechanisms involved in the removal of pollutants using modified fly ash. They highlighted the importance of surface modifications, the role of functional groups, and the application of kinetic and isotherm models in understanding and optimizing the adsorption process (Akpomie et al. 2023, Alaqarbeh 2021)

Influence of pH

pH is a crucial factor in batch mode adsorption, and its effect on phosphate removal was investigated in this study. An adsorption experiment was conducted by changing the pH from 2 to 9. The acid-modified fly ash was used as the adsorbent, with an amount of 0.5 g, 50 ppm concentration, 60 min interaction period at 25°C with a constant agitation speed of 100 rpm. The outcomes indicated that the highest phosphate removal of 90% was attained at pH 5.0, as shown in Fig. 3. Beyond pH 5.0, the adsorption capacity started to decrease. An identical pattern was noticed in other phosphate adsorption studies (Shah et al. 2023). At lower pH values,

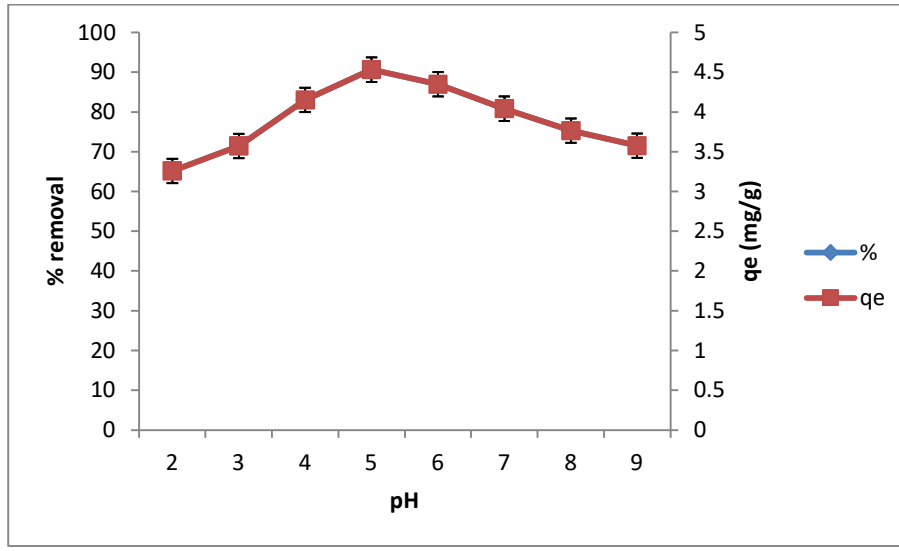

Fig. 3: Influence of pH on phosphate adsorption by AMFA.

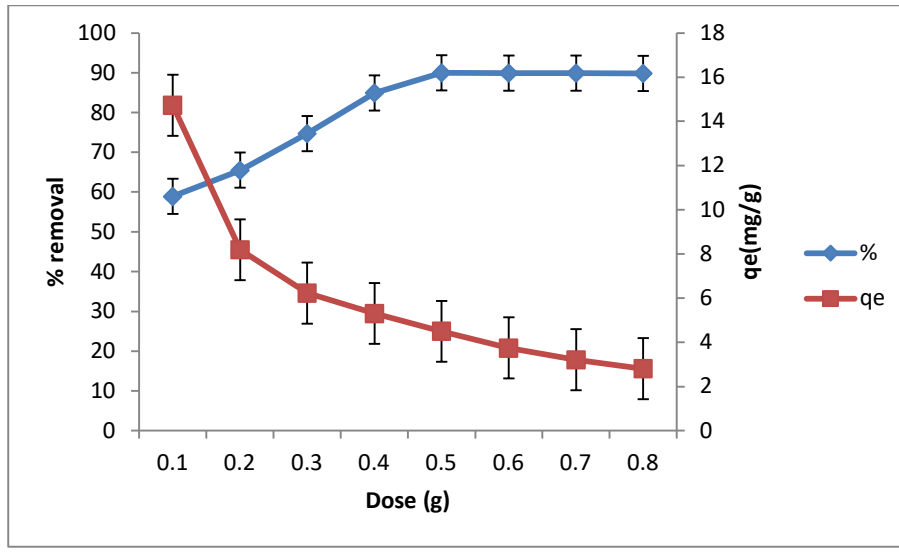

Fig. 4: Influence of adsorbent dosage on phosphate adsorption by AMFA.

the dominant form of phosphate ions was H_3PO_4, which had high solubility in the solutions (Siwek et al. 2019). As the solution pH increased, the concentrations of easily detachable $H_2PO_4^-$ and HPO_4^{2-} forms increased, leading to improved removal efficiency. On the other hand, phosphate ions predominantly existed in the form of PO_4^{3-} at greater pH values, hindering the adsorption process and reducing the removal efficacy (Saleh et al. 2023). In essence, the observed trend can be ascribed to the electrostatic force of attraction between hydrogen ions at low pH conditions and the presence of hydroxyl ions at high pH conditions (Xiong et al. 2017).

Influence of Adsorbent Dosage

The adsorbent dosage plays a significant role in the removal of phosphate from synthetic solutions. Adsorbent dosage ranged from 0.1 to 0.8 g in 50 mL of phosphate solution with a pH of 5.0 and an initial phosphate ion concentration of 50 ppm for an interaction period of 60 min at 25°C. It was noticed that phosphate adsorption by acid-modified fly ash upsurged from 58.92% to 89.96%, as illustrated in Fig. 4. Increasing the adsorbent dosage provides more active binding sites, leading to improved removal efficiency (Ye et

al. 2015). Similarly, when adsorbent dosage was increased, adsorption capacity (q) decreased from 14.73 $mg.g^{-1}$ to 2.80 $mg.g^{-1}$, indicating a negative correlation between phosphate adsorption capacity and adsorbent dosage. However, it is crucial to note that excessive adsorbent dosage, relative to the amount of adsorbate, can result in the unsaturation of adsorption sites, leading to a reduction in uptake capacity (Hu et al. 2015). Similar outcomes were observed when biomass fly ash was used, as reported by Park et al. (2021).

Additionally, more recent studies by Xi et al. (2020) and Wu et al. (2019) have corroborated that increasing the adsorbent dosage improves phosphate removal efficiency. However, this increase can also cause a decrease in specific adsorption capacity due to site saturation. Consequently, a dosage of 0.5 g of AMFA was determined to be the optimal amount for subsequent adsorption experiments.

Influence of Contact Time

Experiments were conducted to study the adsorption of phosphate under various conditions. The contact period ranged from 5 to 80 min, with an initial ion concentration of 50 ppm and an adsorbent dosage of 0.5g.50 mL^{-1}, a solution pH of 5.0 at 25°C (Fig. 5). It was noticed that as the interaction period enhanced, removal efficacy and uptake capacity both upsurged. A noteworthy removal efficacy of phosphate ion by AMFA occurred from 60% to 89% with a rise in time from 5 to 80 min. The maximum uptake capacity was noticed at 4.42 $mg.g^{-1}$ at a time of 80 min. An equilibrium time was established at 30 min. After 30 min, no substantial adsorption took place due to the saturation of binding sites with an increase in time. During the early phases of phosphate sorption, a substantial concentration gradient exists among the film and the accessible pore sites of the adsorbent, resulting in a faster adsorption rate, but in later phases, the adsorption rate declined, which can be attributed to the slower diffusion of the solute ion into the interior of the adsorbent (Chen et al. 2007, Johansson & Gustafsson 2000). Similar results were observed on slag and fly ash for the removal of phosphate ions (Ragheb 2013).

Influence of Initial Phosphate Ion Concentration

The initial phosphate ion concentration has a substantial impact on the adsorption process. To investigate this effect, initial phosphate concentrations ranging from 30 to 150 ppm were studied at an optimum pH of 5.0, with an adsorbent amount of 0.5g.50 mL^{-1}, and an interaction period of 60 min at 25°C. The findings depicted in Fig. 6 that maximum phosphate adsorption took place at 30 ppm and, after that declined as the concentration of phosphate solution upsurged. This decline is attributed to the fact that, at lower concentrations, nearly all phosphate ions were able to bind to the available sites. As the initial phosphate concentration upsurged, these binding sites became saturated, impeding further increase in adsorption capacity at higher concentrations. Furthermore, at higher initial concentrations, the ratio of active sites to phosphate ion concentration decreased with a constant adsorbent dosage and volume of adsorbate (Fetene & Addis 2020). Consequently, there was a reduction in phosphate removal percentage, and these findings are consistent with the conclusions of other studies (Baraka et al. 2012, Trinh et al. 2020).

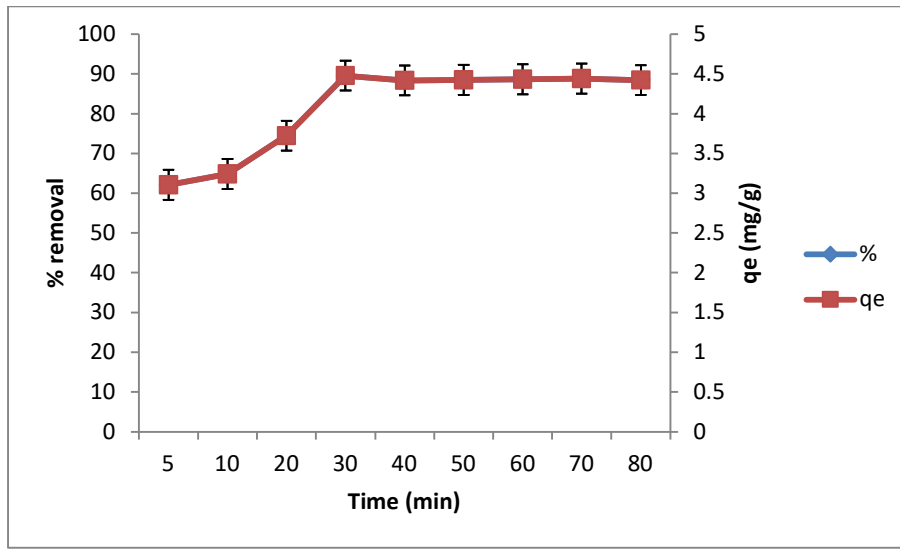

Fig. 5. Influence of contact period on phosphate adsorption by AMFA.

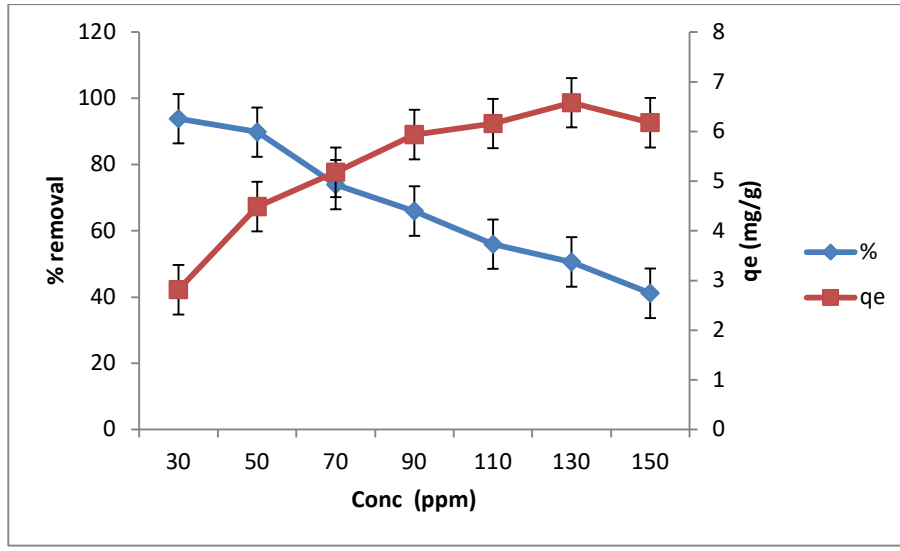

Fig. 6: Influence of initial phosphate ion concentration on phosphate adsorption by AMFA.

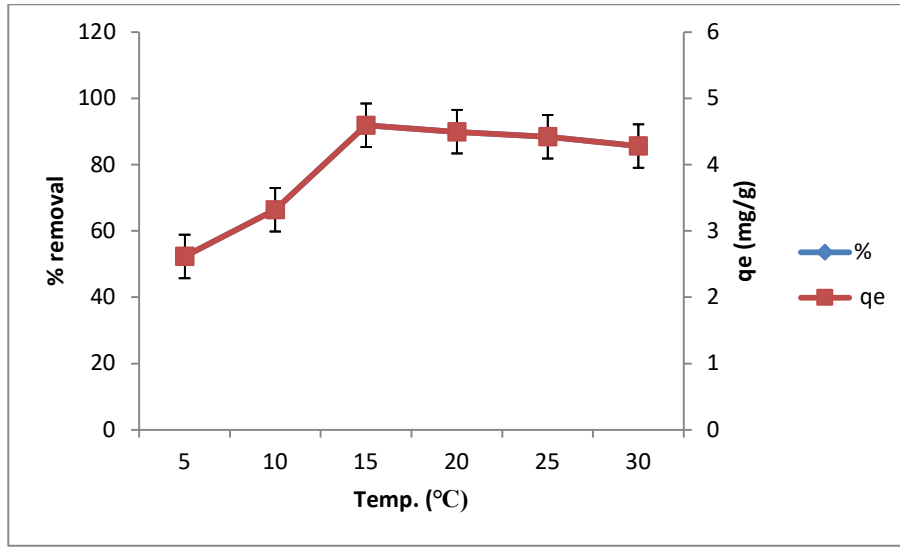

Fig. 7: Influence of temperature on phosphate adsorption by AMFA.

Influence of Temperature

The impact of temperature on phosphate adsorption was explored under different temperature conditions, ranging from 5°C to 30°C. The experiment was performed at 5.0 pH, 0.5 g dose, 60 min of contact time, and a concentration of 30 ppm with a constant stirring of 100 RPM for the adsorption of phosphate ions on acid-modified fly ash. It was determined that removal effectiveness and uptake capacity (q_e) raised to 15°C. The outcomes showed that the highest phosphate removal of 91.88%, followed by 15°C. Fig. 7 illustrated that as the temperature upsurged from 5°C to 30°C, the percentage of phosphate adsorption raised 52.3% to 91.88% and, after that, became stable after 15°C, revealing a preference for phosphate adsorption at lower temperatures (Wu et al. 2019). At elevated temperatures, the molecules in the solution exhibited more vigorous thermal motion, resulting in an increased rate of molecular exchange on the surface of the adsorbent. As a consequence, higher temperatures promoted greater spontaneity in the adsorption process, leading to faster attainment of equilibrium (Al-Harby et al. 2021). A similar pattern was noticed by Sugiyama & Hama (2013).

Adsorption Isotherms

To examine the mechanism and relation between adsorbate and adsorbent, various isotherms, including Langmuir, Freundlich, and Temkin isotherms, were used.

Langmuir Isotherm

The Langmuir isotherm was proposed by Langmuir in 1916 which describes the process of monolayer adsorption on a homogeneous surface. It assumes that the adsorbent surface contains a limited number of uniform sorption binding sites and adsorbate does not migrate inside the surface plane (Langmuir 1916). The highest sorption capacity is calculated using the Langmuir equation, which is shown in eq 3.

$$\frac{C_e}{q_e} = \frac{1}{\mathrm{b}q_m} + \frac{C_e}{q_m} \quad \ldots(3)$$

C_e denotes the equilibrium phosphate concentration (mg.L^{-1}), q_e depicts the adsorbed phosphate concentration at equilibrium (mg/g), and b denotes the Langmuir constant. These constants are derived from both the slope and the intercept of the linear plot of C_e/q_e versus C_e, as presented in Fig. 8.

Separation Factor

Adsorbent surface area and permeability are directly interrelated to the Langmuir constant. As the adsorbent surface area and permeability increase, uptake capacity also rises. Additionally, the value of R_L helps to determine the type of adsorption (Arora et al. 2023).

$$R_L = \frac{1}{(1+\mathrm{b}C_i)} \quad \ldots(4)$$

Table 1. Adsorption isotherm parameters for phosphate on AMFA

Isotherm	Parameters	AMFA
Langmuir	q_m (mg.g^{-1})	46.72
	b	0.01
	R^2	0.14
	R_L	0.83
Freundlich	n	1.189
	K_f(L.g^{-1})	1.11
	R^2	0.86
Temkin	B_T(KJ.moL^{-1})	4.39
	A_T(g.L^{-1})	2.85
	R^2	0.77

R_L represents the separation factor, which is a limitless entity. It is calculated with the help of the Langmuir constant (b) and the initial phosphate concentration (C_i). Depending on the value of R_L, there are four potential scenarios: R_L ranging from 0 to 1 indicates "favorable adsorption", R_L greater than 1 "unfavorable adsorption", R_L equal to 1 signifies "linear adsorption" and R_L equal to 0 implies "irreversible adsorption". AMFA has a separation factor of 0.83 respectively which falls in the range between 0 to 1, indicating favorable adsorption of phosphate.

Fig. 8 and Table 1, the correlation coefficient value was 0.14 for adsorbent acid-modified fly ash, which shows the unfitness of equilibrium data in Langmuir isotherm.

Freundlich Isotherm

Freundlich isotherm model describes the adsorption of molecules on heterogeneous surfaces, where multiple layers

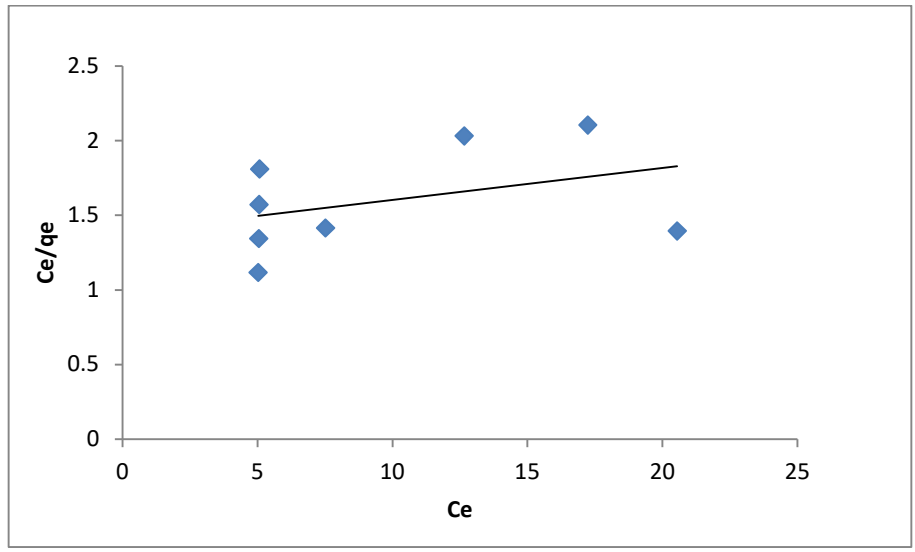

Fig. 8: Langmuir Isotherm: Phosphate Adsorption on AMFA.

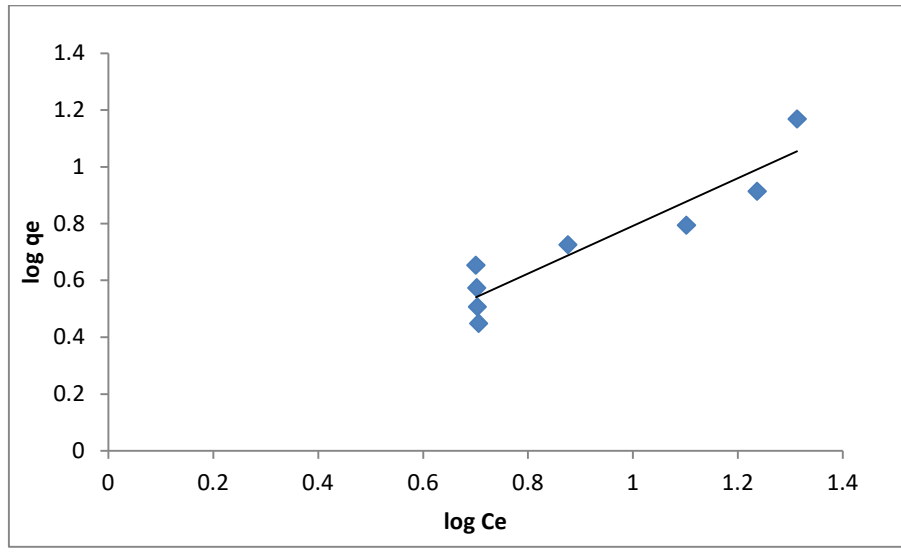

Fig. 9: Freundlich Isotherm: Phosphate Adsorption on AMFA.

of adsorbate can form, and interactions occur among the adsorbed molecules (Freundlich 1907). Freundlich isotherm is presented in a linear form as

$$\log q_e = \log K_f + \frac{1}{n}\log C_e \quad \ldots(5)$$

C_e depicts phosphate equilibrium concentration (mg.L^{-1}), q_e depicts the number of phosphate ions adsorbed at equilibrium (mg.g^{-1}), K_f depicts the Freundlich constant, n depicts the intensity of the adsorption process, and the intercept and slope of the graph among *log* C_e and *log* q_e can be used to determine the values of K_f and n as presented in Fig. 9.

Fig. 9 and Table 1 show that the R^2 value for AMFA was found to be 0.83, which suggests that, Freundlich isotherm better fit into the data. When the value of n is more than 1, it states that it favors the adsorption process. In contrast to the Langmuir isotherm, the adsorption process of the adsorbent was well explained by the Freundlich isotherm. This indicates that the adsorption occurred in multiple layers, suggesting a more complex adsorption mechanism.

Temkin isotherm

Temkin and Pyzhev (1940) introduced the Temkin model, which is used to analyze the adsorption process. According to this, the heat of sorption decreases linearly with temperature instead of following a logarithmic relationship. It may be expressed as:

$$q_e = \frac{R_T}{B_T}\ln A_T + \frac{R_T}{B_T}\ln C_e \quad \ldots(6)$$

C_e depicts the phosphate equilibrium concentration (mg.L^{-1}), q_e depicts the number of phosphate ions adsorbed at equilibrium (mg.g^{-1}), T depicts temperature (Kelvin), R depicts the universally accepted gas constant (8.314 J.moL^{-1}.K^{-1}), B_T depicts the Temkin constant (J.moL^{-1}), A_T depicts constant of Temkin isotherm (g.L^{-1}).

To determine the values of B_T and A_T, a plot of q_e versus ln C_e was plotted for phosphate adsorption on AMFA, as shown in Fig. 10. The plot's slope yields the B_T value, whereas the intercept corresponds to the A_T value.

The Temkin constant (B_T) value indicates the kind of adsorption. When B_T is more than 20 KJ/mol, it means chemical adsorption takes place, and when B_T is less than 20 KJ.moL^{-1}, physical adsorption is significant for the adsorption process. The Temkin constant (B_T) and corresponding R^2 values are 4.39 kJ.moL^{-1} and 0.77 for adsorption of phosphate on AMFA, respectively. Hence, Temkin's study concludes that the adsorption process favors physical adsorption (Table 1).

Adsorption Kinetic Models

The adsorption rate of a solute was determined by studying various kinetic models comprising the pseudo-first-order, pseudo-second-order, and intra-particle diffusion models.

Pseudo-First-Order

Lagergren's pseudo-first-order kinetic equation describes the adsorption of a solute onto an adsorbent (Lagergren 1898) and is given by the following equation:

$$Log\,(q_e - q_t) = \log q_e - \frac{K_1 t}{2.303} \quad \ldots(7)$$

Where q_e represents the equilibrium uptake efficiency (mg.g^{-1}), q_t is the equilibrium uptake efficiency at time t

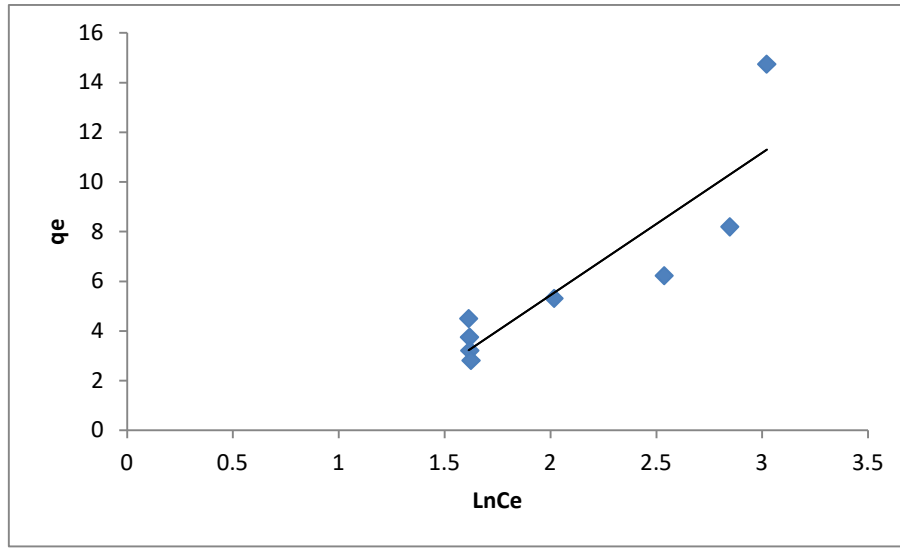

Fig. 10: Temkin Isotherm: Phosphate Adsorption on AMFA.

(min), k_1 depicts the rate constant for pseudo-first-order kinetics (1.min^{-1}), and *t* depicts the adsorption period (min).

A pseudo-first-order kinetic graph was derived by plotting log (q_e - q_t) against time *(t)* (Fig. 11). The values of K_1 and q_e were determined using the slope and intercept of the plot, respectively. The correlation coefficient for acid-modified fly ash is 0.97. The correlation coefficient value over 0.9 indicates that the estimated and experimental adsorption capacities are in strong agreement (Table 2).

Pseudo-Second-Order

The linearized form of the pseudo-second-order equation, as stated by Ho and Mckay (1999), can be conveyed as follows:

$$\frac{t}{q_t} = \frac{1}{K_2 q_e^2} + \frac{t}{q_e} \quad \ldots(8)$$

Here, q_e depicts the equilibrium uptake capacity (mg/g), q_t depicts the adsorption capacity at a specific period (min), and K_2 is the rate constant for the pseudo-second-order model (g.mg^{-1}.min^{-1}). Fig. 12 illustrates a pseudo-second-order kinetic model that was graphed among t/q_t and *t*. The intercept and slope of the plot were used to derive the values of q_e and K_2, respectively. The obtained R^2 value for the adsorbent was 0.997. It was evident from Table 2 that the pseudo-second-order kinetic model was better able to fit the adsorption data. This strong agreement exists because the calculated q_e closely matches the experimental q_{exp}.

Intra-Particle Diffusion

The intra-particle uptake and pore diffusion serve as the foundation in the adsorption process for the intra-particle diffusion concept. To determine the diffusion mechanism, Weber and Morris (1963) found that "intra-particle diffusion of the adsorbate varies proportionately with half power of time during adsorption" and is linearly represented in eq 9:

$$q_t = k_i\sqrt{t} + x_i \quad \ldots(9)$$

Here x_i represents the wideness of the border layer (mg.g^{-1}), and k_i (mg.g^{-1} min$^{0.5}$) is the intra-particle diffusion rate constant. Using the intra-particle diffusion model's plot between q_t and *t*, the values of x_i and k_i were determined from the intercept and slope (Fig. 13). According to Singh and Bhateria 2020, the wideness of the border layer is dependent on the greater value of x_i. The values of x_i and R^2 attained 2.7891 mg/g and 0.79 for AMFA, respectively (Table 2).

Based on the kinetic findings, it was determined that the pseudo-second-order kinetic model provided a more precise

Table 2. Kinetic model parameters for phosphate adsorption on AMFA

Kinetic models	Parameters	AMFA
Experimental adsorption capacity	$q_{e\ exp}$ (mg/g)	4.47
Pseudo-first-order kinetics	$q_{e\ cal}$ (mg/g)	1.04
	K_1 (1/ min)	0.52
	R^2	0.97
Pseudo-second-order kinetics	$q_{e\ cal}$ (mg/g)	4.64
	K_2 (g/mg/min)	0.06
	R^2	0.997
Intra-particle diffusion	K_i [mg/(g min$^{0.5}$)]	0.2153
	x_i (mg/g)	2.7891
	R^2	0.7906

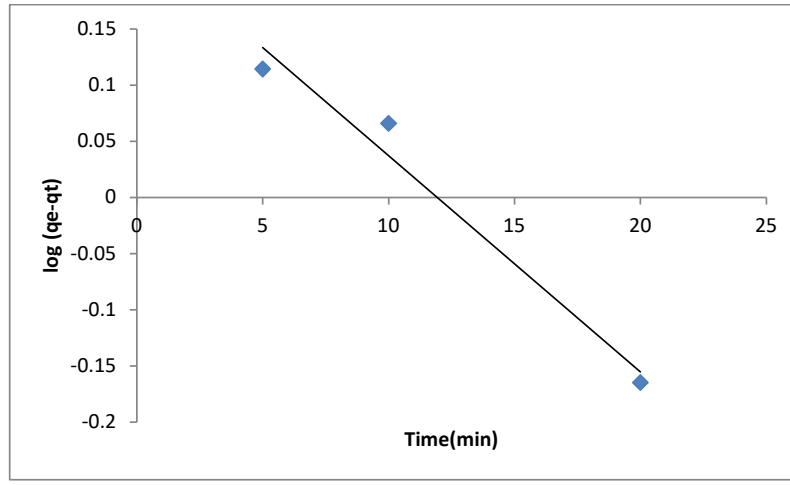

Fig. 11: Pseudo-first-order plot for phosphate adsorption on AMFA.

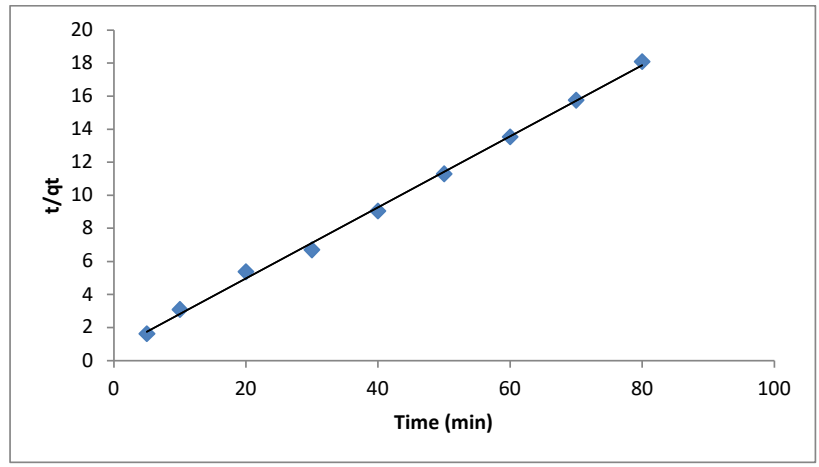

Fig. 12: Pseudo-second-order plot for phosphate adsorption on AMFA.

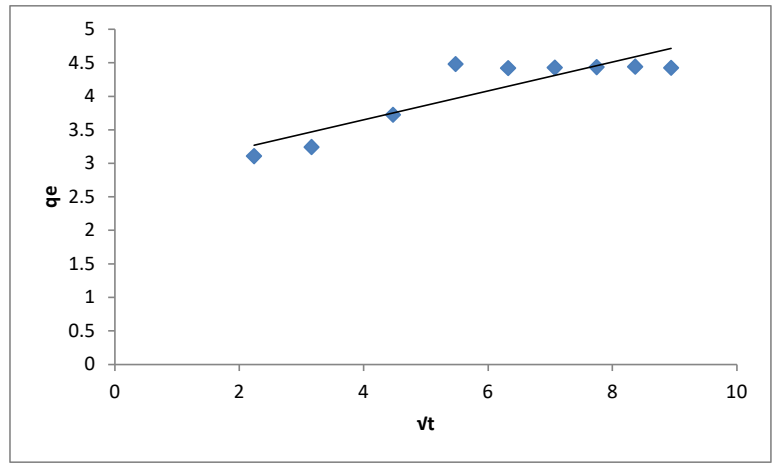

Fig. 13: Intra-particle diffusion plot for phosphate adsorption on AMFA.

fit to the adsorption data rather than the pseudo-first-order kinetic model.

Thermodynamic Studies

Adsorption thermodynamics were employed to determine the sort of adsorption occurring in the phosphate adsorption process with acid-modified fly ash. As per the findings of Ngah and Hanafiah (2008), a reduction in ΔG with rising temperature suggests that the sorption process would be possible and spontaneous. ΔG is calculated using eq 10:

$$\Delta G = -RT ln\, K \quad \ldots(10)$$

Where T depicts temperature in K (Kelvin), and R depicts the gas constant (8.314 J/mol/K). Diverse temperatures considered for the thermodynamic study were 278 K, 283 K, 288 K, 293 K, and 303 K. The Van't Hoff interaction was utilized to govern the thermodynamic parameters ΔH° and ΔS°. The Van't Hoff graph was plotted between lnK_d and 1000/T (Fig. 14). Both the slope and intercept of the plot were utilized to calculate ΔH° and ΔS°.

$$lnK_d = \frac{\Delta S^\circ}{R} - \frac{\Delta H^\circ}{RT} \quad \ldots(11)$$

$$\Delta G^\circ = \Delta H^\circ - T\Delta S^\circ \quad \ldots(12)$$

where T depicts temperature (K), $K_d = q_e/C_e$ depicts distribution coefficient, R depicts the universally accepted gas constant (8.314 J.moL^{-1}.K^{-1}), C_e depicts the equilibrium phosphate concentration (mg.L^{-1}), q_e represents the number of phosphate ions adsorbed at equilibrium (mg.g^{-1}), ΔG determines the spontaneity of the adsorption process, with

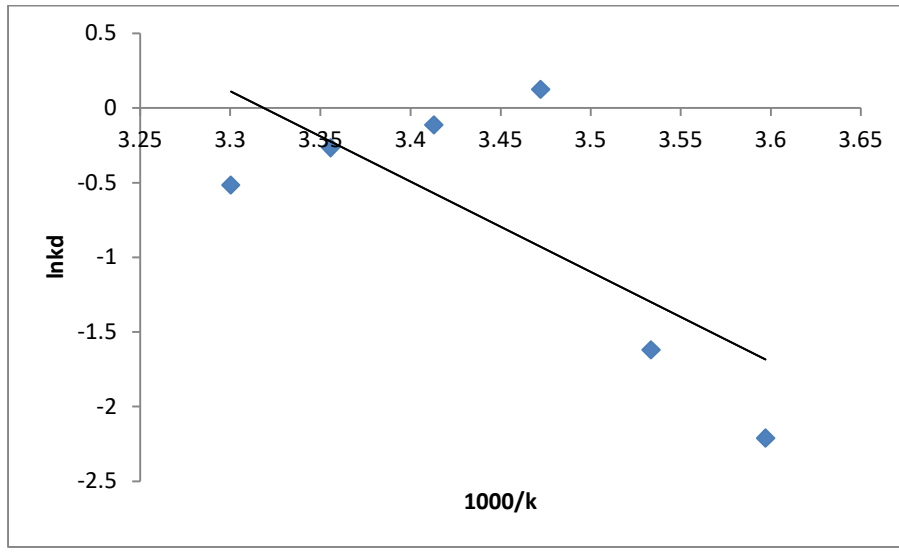

Fig. 14: Van't Hoff Analysis of Phosphate Adsorption on AMFA.

Table 3. Thermodynamic factors for the adsorption of phosphate on AMFA

Adsorbent	ΔH° (kJ/mol)	ΔS° (KJ/mol/K)	ΔG° (KJ/mol)					
			278 K	283K	288K	293K	298K	303K
AMFA	50.25	0.166	4.11	3.27	2.45	1.62	0.79	-0.048

Table 4. Maximum uptake capacities of different industrial waste-based adsorbents

Adsorbate	Adsorbent	Maximum sorption capacity(q_e) mg/g	References
Phosphate	Electric arc furnace steel slag	2.2	Drizo et al. 2006
Phosphate	Crushed brick with iron oxide coating	1.8	Boujelben et al. 2008
Phosphate	Red mud	0.5	Castaldi et al. 2010
Phosphate	HCl treated red mud	0.58	Huang et al. 2008
Phosphate	Fly ash	3.34	Yu et al. 2015
Phosphate	Acid modified fly ash (AMFA)	4.47	Current study

a positive value indicating a non-spontaneous process and a negative value indicating a spontaneous process. ΔH depicts whether the process is exothermic or endothermic. A positive ΔH represents an endothermic process, while a negative ΔH shows an exothermic process. Positive and negative values of ΔS indicate an increase or decrease in the degree of randomness at the solid-liquid interface, respectively.

Table 3 displays the findings from the thermodynamic study. The positive values of all the thermodynamic parameters (ΔH^o, ΔS^o, and ΔG^o) illustrate that the adsorption process is endothermic and non-spontaneous at lower temperatures and spontaneous at higher temperatures.

Comparison and Analysis of Different Adsorbents

Table 4 analyzes and compares the maximum sorption capacities of diverse industrial waste-based adsorbents for the adsorption of phosphate. Various adsorbents such as electric arc furnace steel slag (Drizo et al. 2006), iron oxide coated crushed brick (Boujelben et al. 2008), red mud (Castaldi et al. 2010), HCl treated red mud (Huang et al. 2008) and fly ash (Yu et al. 2015) have been used for confiscation of phosphate from synthetic solutions.

CONCLUSIONS

This study focused on evaluating the capability of acid-modified fly ash (AMFA) to eliminate phosphate from synthetic solutions. The results revealed that AMFA exhibited effective phosphate removal, with a maximal sorption capacity of 4.47 $mg.g^{-1}$. The sorption of phosphate remained relatively stable under acidic solution pH conditions but significantly decreased as the pH approached strongly alkaline levels. Thermodynamic studies indicated that the rate of phosphate sorption on AMFA increased with rising temperatures, indicating an endothermic and non-spontaneous process. The kinetic data was well defined by the pseudo-second-order model. Both the Freundlich and Temkin isotherms provided good fits for the equilibrium data, suggesting multilayer adsorption and possible interaction between the adsorbate and adsorbent surface. Overall, this investigation demonstrated the effective use of AMFA for phosphate removal from synthetic solutions. Additionally, the study showed that AMFA could be potentially utilized for repeated regeneration of phosphate from synthetic solutions, further highlighting its applicability as an adsorbent material in water treatment processes.

REFERENCES

Ahmaruzzaman, M., 2010. A review on the utilization of fly ash. *Progress in Energy and Combustion Science, 36(3)*, pp.327-363. [DOI]

Ahmaruzzaman, M., 2011. Industrial wastes as low-cost potential adsorbents for the treatment of wastewater laden with heavy metals. *Advances in Colloid and Interface Science, 166(1-2)*, pp.36-59. [DOI]

Akpomie, K.G., Conradie, J., Adegoke, K.A., Oyedotun, K.O., Ighalo, J.O., Amaku, J.F., Olisah, C., Adeola, A.O. and Iwuozor, K.O., 2023. Adsorption mechanism and modeling of radionuclides and heavy metals onto ZnO nanoparticles: a review. *Applied Water Science, 13(1)*, p.20. [DOI]

Alaqarbeh, M., 2021. Adsorption phenomena: definition, mechanisms, and adsorption types: short review. *RHAZES: Green and Applied Chemistry, 13*, pp.43-51. [DOI]

Al-Harby, N.F., Albahly, E.F. and Mohamed, N.A., 2021. Kinetics, isotherm, and thermodynamic studies for efficient adsorption of Congo Red dye from aqueous solution onto novel cyanoguanidine-modified chitosan adsorbent. *Polymers, 13(24)*, p.4446. [DOI]

American Public Health Association, 1926. *Standard Methods for the Examination of Water and Wastewater (Vol. 6).* American Public Health Association.

Arora, D., Arora, A., Singh, A., Agarwal, R., Bala, R. and Kumar, S., 2023. Evaluating the applicability of *Brachiaria mutica* (Forssk.)(Paragrass) and *Cyperus rotundus* L.(Nutgrass) as bioadsorbents to remove Cr (VI): isotherms, kinetics, and thermodynamic studies. *Sustainable Water Resources Management, 9(5)*, p.168. [DOI]

Baraka, A.M., El-Tayieb, M.M., El-Shafai, M. and Mohamed, N.Y., 2012. Sorptive removal of phosphate from wastewater using activated red mud. *Journal of Environmental Science and Technology, 10(1)*, pp.55-63.

Boujelben, N., Bouzid, J., Elouear, Z., Feki, M., Jamoussi, F. and Montiel, A., 2008. Phosphorus removal from aqueous solution using iron-coated natural and engineered sorbents. *Journal of Hazardous Materials, 151(1)*, pp.103-110. [DOI]

Buema, G., Harja, M., Lupu, N., Chiriac, H., Forminte, L., Ciobanu, G., Bucur, D. and Bucur, R.D., 2021. Adsorption performance of modified fly ash for copper ion removal from aqueous solution. *Water, 13(2)*, p.207. [DOI]

Castaldi, P., Silvetti, M., Garau, G. and Deiana, S., 2010. Influence of the pH on the accumulation of phosphate by red mud (a bauxite ore processing waste). *Journal of Hazardous Materials, 182(1-3)*, pp.266-272. [DOI]

Chen, J., Kong, H., Wu, D., Chen, X., Zhang, D. and Sun, Z., 2007. Phosphate immobilization from aqueous solution by fly ashes in relation to their composition. *Journal of Hazardous Materials, 139(2)*, pp.293-300. [DOI]

De Gisi, S., Lofrano, G., Grassi, M. and Notarnicola, M., 2016. Characteristics and adsorption capacities of low-cost sorbents for wastewater treatment: a review. *Sustainable Materials and Technologies, 9*, pp.10-40. [DOI]

Drizo, A., Forget, C., Chapuis, R.P. and Comeau, Y., 2006. Phosphorus removal by electric arc furnace steel slag and serpentinite. *Water Research, 40(8)*, pp.1547-1554. [DOI]

Fetene, Y. and Addis, T., 2020. Adsorptive removal of phosphate from wastewater using Ethiopian rift pumice: Batch experiment. *Air, Soil and Water Research, 13*, p.1178622120969658. [DOI]

Freundlich, H., 1907. Über die adsorption in lösungen. *Zeitschrift für Physikalische Chemie, 57(1)*, pp.385-470.

Ho, Y.S. and McKay, G., 1999. Pseudo-second order model for sorption processes. *Process Biochemistry, 34(5)*, pp.451-465. [DOI]

Hosseinpour, S., Hejazi-Mehrizi, M., Hashemipour, H. and Farpoor, M.H., 2023. Adsorptive removal of phosphorus from aqueous solutions using natural and modified coal solid wastes. *Water Science & Technology, 87(6)*, pp.1376-1392. [DOI]

Hu, Q., Chen, N., Feng, C. and Hu, W., 2015. Nitrate adsorption from aqueous solution using granular chitosan-Fe3+ complex. *Applied Surface Science, 347*, pp.1-9. [DOI]

Huang, W., Wang, S., Zhu, Z., Li, L., Yao, X., Rudolph, V. and Haghseresht, F., 2008. Phosphate removal from wastewater using red mud. *Journal of Hazardous Materials, 158(1)*, pp.35-42. [DOI]

Irawan, C., Atikah, A. and Rumhayati, B., 2014. Adsorption of iron by fly ash adsorbent of coal. *The Journal of Pure and Applied Chemistry Research, 3(3)*, p.88.

Johansson, L. and Gustafsson, J.P., 2000. Phosphate removal using blast furnace slags and opoka-mechanisms. *Water Research, 34(1)*, pp.259-265. [DOI]

Karaca, S., Gürses, A., Ejder, M. and Açıkyıldız, M., 2004. Kinetic modeling of liquid-phase adsorption of phosphate on dolomite. *Journal of Colloid and Interface Science, 277(2)*, pp.257-263. [DOI]

Küçük, İ. and Üstündağ, P., 2024. Adsorption performance of acidic modified fly ash: Box–Behnken design. *Journal of the Turkish Chemical Society Section A: Chemistry, 11(2)*, pp.699-708. [DOI]

Lagergren, S., 1898. About the theory of so-called adsorption of soluble substances. *Fictitious Journal of Chemical Science, 10(1)*, pp.100-120.

Langmuir, I., 1916. The constitution and fundamental properties of solids and liquids. Part I. Solids. *Journal of the American Chemical Society, 38(11)*, pp.2221-2295.

Loganathan, P., Vigneswaran, S., Kandasamy, J. and Bolan, N.S., 2014. Removal and recovery of phosphate from water using sorption. *Critical Reviews in Environmental Science and Technology, 44(8)*, pp.847-907. [DOI]

Neufeld, R.D. and Thodos, G., 1969. Removal of orthophosphates from aqueous solutions with activated alumina. *Environmental Science & Technology, 3(7)*, pp.661-667. [DOI]

Ngah, W.W. and Hanafiah, M.A.K.M., 2008. Adsorption of copper on rubber (Hevea brasiliensis) leaf powder: Kinetic, equilibrium and thermodynamic studies. *Biochemical Engineering Journal, 39(3)*, pp.521-530. [DOI]

Park, J.H., Hwang, S.W., Lee, S.L., Lee, J.H. and Seo, D.C., 2021. Sorption behavior of phosphate by fly ash discharged from biomass thermal power plant. *Applied Biological Chemistry, 64(1)*, p.43.

Ragheb, S.M., 2013. Phosphate removal from aqueous solution using slag and fly ash. *HBRC Journal, 9(3)*, pp.270-275. [DOI]

Recepoglu, Y.K., Goren, A.Y., Orooji, Y. and Khataee, A., 2022. Carbonaceous materials for removal and recovery of phosphate species: Limitations, successes, and future improvement. *Chemosphere, 287*, p.132177. [DOI]

Ren, X. and Sancaktar, E., 2019. Use of fly ash as eco-friendly filler in synthetic rubber for tire applications. *Journal of Cleaner Production, 206*, pp.374-382. [DOI]

Saad Algarni, T. and Al-Mohaimeed, A.M., 2022. Water purification by adsorption of pigments or pollutants via metal oxide. *Journal of King Saud University-Science, 34(8)*, p.102339. [DOI]

Saleh, M., Alterkaoui, A., Ozdemir, N.C., Arslan, H., Bilici, Z. and Dizge, N., 2024. Adsorption of phosphate ions and reactive red 180 from aqueous solution using thermally activated lemon peel waste. *International Journal of Environmental Science and Technology, 21(2)*, pp.1683-1696. [DOI]

Shah, K.H., Fareed, M., Waseem, M., Shahida, S., Hatshan, M.R., Sarfraz, S., Batool, A., Fahad, M., Ahmad, T., Shah, N.S. and Ha, K., 2023. Tea-waste-mediated magnetic oxide nanoparticles as a potential low-cost adsorbent for phosphate (PO_4^{3-}) anion remediation. *Water, 15(20)*, p.3541. [DOI]

Sharma, P.K., Ayub, S. and Tripathi, C.N., 2016. Isotherms describing physical adsorption of Cr (VI) from aqueous solution using various agricultural wastes as adsorbents. *Cogent Engineering, 3(1)*, p.1186857. [DOI]

Singh, N., Mithulraj, M. and Arya, S., 2019. Utilization of coal bottom ash in recycled concrete aggregates based self-compacting concrete blended with metakaolin. *Resources, Conservation and Recycling, 144*, pp.240-251. [DOI]

Singh, R. and Bhateria, R., 2020. Experimental and modeling process optimization of lead adsorption on magnetite nanoparticles via isothermal, kinetics, and thermodynamic studies. *ACS Omega, 5(19)*, pp.10826-10837. [DOI]

Siwek, H., Bartkowiak, A. and Włodarczyk, M., 2019. Adsorption of phosphates from aqueous solutions on alginate/goethite hydrogel composite. *Water, 11(4)*, p.633. [DOI]

Sugiyama, S. and Hama, T., 2013. Effects of water temperature on phosphate adsorption onto sediments in an agricultural drainage canal in a paddy-field district. *Ecological Engineering*, 61, pp.94-99. [DOI]

Sun, J., Yang, Q., Wang, D., Wang, S., Chen, F., Zhong, Y., Yi, K., Yao, F., Jiang, C., Li, S. and Li, X., 2017. Nickel toxicity to the performance and microbial community of enhanced biological phosphorus removal system. *Chemical Engineering Journal*, 313, pp.415-423. [DOI]

Temkin, M.J. and Pyzhev, V., 1940. Recent Modifications to Langmuir Isotherms. [Fictitious details].

Trinh, V.T., Nguyen, T.M.P., Van, H.T., Hoang, L.P., Nguyen, T.V., Ha, L.T., Vu, X.H., Pham, T.T., Nguyen, T.N., Quang, N.V. and Nguyen, X.C., 2020. Phosphate adsorption by silver nanoparticles-loaded activated carbon derived from tea residue. *Scientific Reports*, 10(1), p.3634. [DOI]

Usman, M., Anastopoulos, I., Hamid, Y. and Wakeel, A., 2023. Recent trends in the use of fly ash for the adsorption of pollutants in contaminated wastewater and soils: Effects on soil quality and plant growth. *Environmental Science and Pollution Research*, 30(60), pp.124427-124446. [DOI]

Wang, D., Yang, G., Li, X., Zheng, W., Wu, Y., Yang, Q. and Zeng, G., 2012. Inducing mechanism of biological phosphorus removal driven by the aerobic/extended-idle regime. *Biotechnology and Bioengineering*, 109(11), pp.2798-2807. [DOI]

Wang, W., Qi, L. and Zhang, J., 2024. Specific resistance and adsorption performance of acid-modified fly ash for escaped ammonia in flue gas. *Journal of Hazardous Materials*, 465, p.133072. [DOI]

Weber Jr, W.J. and Morris, J.C., 1963. Kinetics of adsorption on carbon from solution. *Journal of the Sanitary Engineering Division*, 89(2), pp.31-59. [DOI]

Wu, B., Wan, J., Zhang, Y., Pan, B. and Lo, I.M., 2019. Selective phosphate removal from water and wastewater using sorption: Process fundamentals and removal mechanisms. *Environmental Science & Technology*, 54(1), pp.50-66. [DOI]

Wulandari, W.R., Saefumillah, A. and Yunarti, R.T., 2019, July. Modification of fly ash using acids and alkali by hydrothermal method and its application as adsorbent material for phosphate adsorption in aquatic systems. *IOP Conference Series: Materials Science and Engineering*, 902(1), p.012034. IOP Publishing. [DOI]

Xi, H., Li, Q., Yang, Y., Zhang, J., Guo, F., Wang, X., Xu, S. and Ruan, S., 2021. Highly effective removal of phosphate from complex water environment with porous Zr-bentonite alginate hydrogel beads: Facile synthesis and adsorption behavior study. *Applied Clay Science*, 201, p.105919. [DOI]

Xie, T., Mo, C., Li, X., Zhang, J., An, H., Yang, Q., Wang, D., Zhao, J., Zhong, Y. and Zeng, G., 2017. Effects of different ratios of glucose to acetate on phosphorus removal and microbial community of enhanced biological phosphorus removal (EBPR) system. *Environmental Science and Pollution Research*, 24, pp.4494-4505. [DOI]

Xiong, W., Tong, J., Yang, Z., Zeng, G., Zhou, Y., Wang, D., Song, P., Xu, R., Zhang, C. and Cheng, M., 2017. Adsorption of phosphate from aqueous solution using iron-zirconium modified activated carbon nanofiber: Performance and mechanism. *Journal of Colloid and Interface Science*, 493, pp.17-23. [DOI]

Xu, R., Lyu, T., Wang, L., Yuan, Y., Zhang, M., Cooper, M., Mortimer, R.J., Yang, Q. and Pan, G., 2022. Utilization of coal fly ash waste for effective recapture of phosphorus from waters. *Chemosphere*, 287, p.132431. [DOI]

Yang, Q., Wang, X., Luo, W., Sun, J., Xu, Q., Chen, F., Zhao, J., Wang, S., Yao, F., Wang, D. and Li, X., 2018. Effectiveness and mechanisms of

phosphate adsorption on iron-modified biochars derived from waste activated sludge. *Bioresource Technology*, 247, pp.537-544. [DOI]

Yao, Y., Gao, B., Inyang, M., Zimmerman, A.R., Cao, X., Pullammanappallil, P. and Yang, L., 2011. Removal of phosphate from aqueous solution by biochar derived from anaerobically digested sugar beet tailings. *Journal of Hazardous Materials*, 190(1-3), pp.501-507. [DOI]

Ye, J., Cong, X., Zhang, P., Hoffmann, E., Zeng, G., Wu, Y., Zhang, H. and Fan, W., 2015. Phosphate adsorption onto granular-acid-activated-neutralized red mud: parameter optimization, kinetics, isotherms, and mechanism analysis. *Water, Air, & Soil Pollution*, 226, pp.1-10. [DOI]

Yeoman, S., Stephenson, T., Lester, J.N. and Perry, R., 1988. The removal of phosphorus during wastewater treatment: a review. *Environmental Pollution*, 49(3), pp.183-233. [DOI]

Yin, Q., Zhang, B., Wang, R. and Zhao, Z., 2017. Biochar as an adsorbent for inorganic nitrogen and phosphorus removal from water: a review. *Environmental Science and Pollution Research*, 24, pp.26297-26309. [DOI]

Yu, J., Liang, W., Wang, L., Li, F., Zou, Y. and Wang, H., 2015. Phosphate removal from domestic wastewater using thermally modified steel slag. *Journal of Environmental Sciences*, 31, pp.81-88. [DOI]

Zhang, X., Lin, X., He, Y., Chen, Y., Zhou, J. and Luo, X., 2018. Adsorption of phosphorus from slaughterhouse wastewater by carboxymethyl konjac glucomannan loaded with lanthanum. *International Journal of Biological Macromolecules*, 119, pp.105-115. [DOI]

Zhou, J., Leavitt, P.R., Zhang, Y. and Qin, B., 2022. Anthropogenic eutrophication of shallow lakes: is it occasional? *Water Research*, 221, p.118728. DOI